

1 INCLUDING THE $\mathcal{D}_{H\beta}$ PARAMETER

Another interesting bi-variate relation is found between the L_{bol}/L_{Edd} which is a function of (a) the shape of the broad-line profile ($\mathcal{D}_{H\beta} = FWHM/\sigma_{H\beta}$), and (b) the parameter R_{FeII} . The $\mathcal{D}_{H\beta}$ is better known as the line-width ratio (see e.g., Kollatschny and Zetzl, 2013), i.e. the ratio between the full-width at half maximum (FWHM) of the emission line (here, $H\beta$) and the corresponding dispersion in the $H\beta$ line ($\sigma_{H\beta}$). In Du et al. (2016), the authors provided a novel relation that is stated as the fundamental relation for the BLR and has the form,

$$\log \lambda_{Edd} = \alpha' + \beta \mathcal{D}_{H\beta} + \gamma R_{FeII} \quad (14)$$

The values taken by the coefficients are: $\alpha' = 0.31 \pm 0.30$, $\beta = -0.82 \pm 0.11$, and $\gamma = 0.80 \pm 0.20$.

The monochromatic luminosity at 5100\AA (L_{5100}) can be re-written using the black hole mass (M_{BH}) and the Eddington ratio, i.e., $\lambda_{Edd} = L_{bol}/L_{Edd}$. Again, we have two versions with the inclusion of the bolometric correction factor. Assuming the fixed $k_{bol} = 9.26$ (Richards et al., 2006), we have

$$\log(L_{5100}) = \log\left(\frac{L_{bol}}{9.26}\right) = \log\left(\frac{\lambda_{Edd} L_{Edd}}{9.26}\right) = \log(\lambda_{Edd}) + \log(M_{BH}) + 37.13375956 \quad (15)$$

While on the other hand assuming the variable k_{bol} (Netzer, 2019), we have

$$\log(L_{5100}) = \log\left(\frac{L_{bol}}{k_{bol}}\right) = 1.25 [\log(\lambda_{Edd}) + \log(M_{BH})] + 35.12288819 \quad (16)$$

Incorporating this BLR fundamental plane relation in our previously obtained analytical relations with $\log Un_H$ we get the following relations:

Applying Equation 14 in Equation 6 with Equation 15, we have

$$\log(Un_H) = 9.694 - 0.084 \log\left(\frac{M_{BH}}{10^8 M_{\odot}}\right) + 0.069 \mathcal{D}_{H\beta} - 0.067 R_{FeII} \quad (17)$$

Applying Equation 14 in Equation 7 with Equation 16, we have

$$\log(Un_H) = 9.621 - 0.355 \log\left(\frac{M_{BH}}{10^8 M_{\odot}}\right) + 0.291 \mathcal{D}_{H\beta} - 0.284 R_{FeII} \quad (18)$$

Applying Equation 14 in Equation 9 with Equation 15, we have

$$\log(Un_H) = 9.769 + 0.1 \log\left(\frac{M_{BH}}{10^8 M_{\odot}}\right) - 0.082 \mathcal{D}_{H\beta} + 0.78 R_{FeII} \quad (19)$$

Applying Equation 14 in Equation 10 with Equation 16, we have

$$\log(U_{n_H}) = 9.709 - 0.125 \log\left(\frac{M_{\text{BH}}}{10^8 M_{\odot}}\right) + 0.103\mathcal{D}_{H\beta} + 0.6R_{\text{FeII}} \quad (20)$$

The estimates from the above analytical relations are summarised in Table S1. Similar to Table 1, we report the estimates for all the cases accounting for the appropriate χ values for the two sources in the last two columns in Table S1.

Table S1. Estimates for $\log(U_{n_H})$ for the various relations considered in this paper including the $\mathcal{D}_{H\beta}$ parameter

Radius-Luminosity relation	Bolometric Correction	$\log(U_{n_H})$	NGC 5548 ^a	I Zw 1 ^b	NGC 5548 ^c	I Zw 1 ^d
Bentz et al. (2013)	Richards et al. (2006)	$9.694 - 0.084 \log\left(\frac{M_{\text{BH}}}{10^8 M_{\odot}}\right) + 0.069\mathcal{D}_{H\beta} - 0.067R_{\text{FeII}}$	9.895	9.647	10.110	9.027
	Netzer (2019)	$9.621 - 0.355 \log\left(\frac{M_{\text{BH}}}{10^8 M_{\odot}}\right) + 0.291\mathcal{D}_{H\beta} - 0.284R_{\text{FeII}}$	10.467	9.420	10.682	8.800
Du and Wang (2019)	Richards et al. (2006)	$9.769 + 0.11 \log\left(\frac{M_{\text{BH}}}{10^8 M_{\odot}}\right) - 0.082\mathcal{D}_{H\beta} + 0.78R_{\text{FeII}}$	9.600	10.959	9.815	10.339
	Netzer (2019)	$9.709 - 0.125 \log\left(\frac{M_{\text{BH}}}{10^8 M_{\odot}}\right) + 0.103\mathcal{D}_{H\beta} + 0.6R_{\text{FeII}}$	10.078	10.772	10.293	10.152

^a denotes for the case with $\chi=0.5$ which is used to estimate values for NGC 5548 and I Zw 1 in columns 4 and 5, respectively. Black hole mass (M_{BH}) for: ^a NGC 5548 = $(5.2 \pm 1.3) \times 10^7 M_{\odot}$ (Fausnaugh et al., 2016); ^b I Zw 1 = $(8.61 \pm 1.50) \times 10^7 M_{\odot}$ (Martínez-Aldama et al., 2021b). The M_{BH} is estimated using the spectral properties obtained from Persson (1988). These are consistent with their respective SEDs considered in this paper. The corresponding $\mathcal{D}_{H\beta}$ and R_{FeII} for (a) NGC 5548 are 2.66 ± 0.13 , and 0.1 ± 0.02 (Du and Wang, 2019), respectively; and for (b) I Zw 1 are 0.809 ± 0.13 , and 1.619 ± 0.060 (Marziani et al. 2021, submitted), respectively. ^c uses the $\chi=0.82$ as reported by CLOUDY for NGC 5548, ^d uses the $\chi=0.12$ as reported by CLOUDY for I Zw 1, keeping other parameters identical as before.

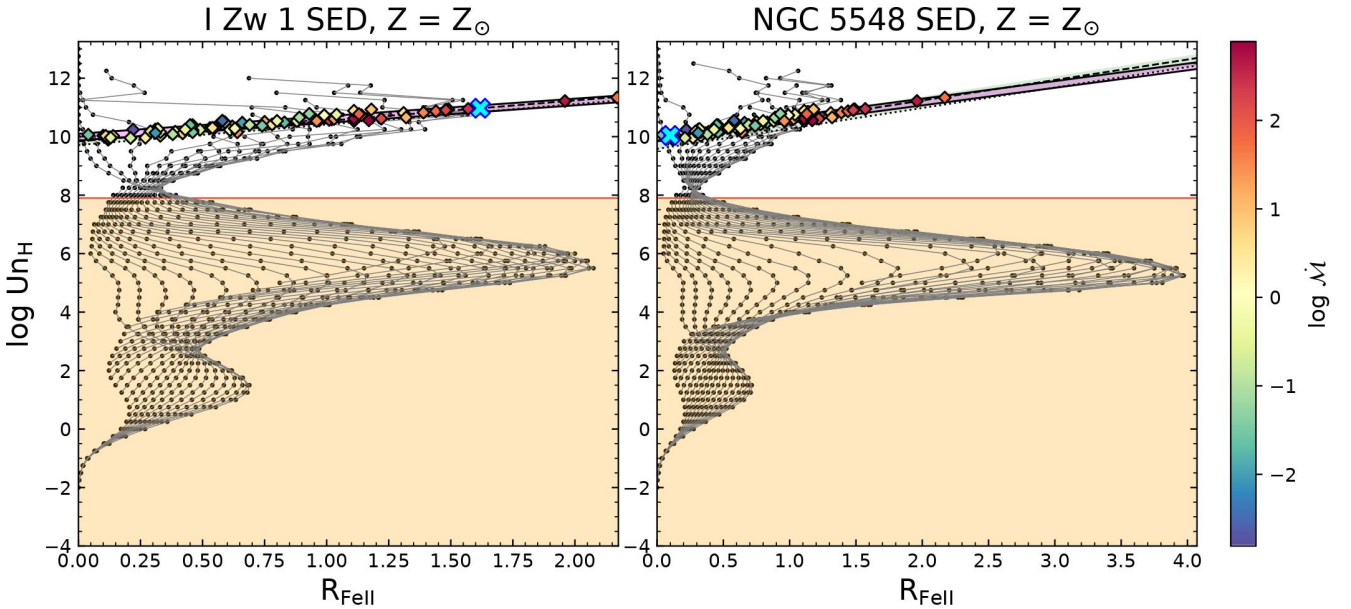


Figure S1. Similar to Figure 7 but with the inclusion of the $\mathcal{D}_{H\beta}$ in the analytical prescription. The panels include the full range of the $\mathcal{D}_{H\beta}$ as per min-max range from the histogram shown in Figure 4. The U_{n_H} estimates for the observed sample is based on the luminosity-dependent k_{bol} and R_{FeII} -based $R_{H\beta} - L_{5100}$ relation as shown in Table S1. The blue cross in each panel shows the location of the respective sources from the estimates tabulated in the last row of Table S1.

Table S2 Spectral and derived properties of reverberation-mapped AGNs

Source	$\log L_{5100}$ [erg s ⁻¹]	$\log M_{BH}$ [M_{\odot}]	$\log \dot{M}$	R_{FeII}	$\mathcal{D}_{H\beta}$
Mrk 335	43.76±0.07	6.93 ^{+0.1} _{-0.11}	1.27 ^{+0.18} _{-0.17}	0.62±0.124	1.27±0.05
PG 0026+129	44.97±0.02	8.15 ^{+0.09} _{-0.13}	0.65 ^{+0.28} _{-0.2}	0.33±0.066	1.46±0.09
PG 0052+251	44.81±0.03	8.64 ^{+0.11} _{-0.14}	-0.59 ^{+0.31} _{-0.25}	0.12±0.024	2.31±0.05
Fairall9	43.98±0.04	8.09 ^{+0.07} _{-0.12}	-0.71 ^{+0.31} _{-0.21}	0.49±0.098	2.56±0.03
Mrk 590	43.5±0.21	7.55 ^{+0.07} _{-0.08}	-0.41 ^{+0.36} _{-0.36}	0.45±0.09	1.39±0.07
Mrk 1044	43.1±0.1	6.45 ^{+0.12} _{-0.13}	1.22 ^{+0.4} _{-0.41}	0.99±0.198	1.54±0.03
3C 120	44±0.1	7.79 ^{+0.15} _{-0.15}	-0.07 ^{+0.3} _{-0.3}	0.39±0.078	1.86±0.05
IRAS 04416+1215	44.47±0.03	6.78 ^{+0.31} _{-0.06}	2.63 ^{+0.16} _{-0.67}	1.96±0.392	1.44±0.06
Ark 120	43.87±0.25	8.47 ^{+0.07} _{-0.08}	-1.7 ^{+0.41} _{-0.41}	0.83±0.166	1.65±0.01
MCG +08-11-011	43.33±0.11	7.72 ^{+0.04} _{-0.05}	-0.96 ^{+0.25} _{-0.28}	0.29±0.058	1.55±0.11
Mrk 374	43.77±0.04	7.86 ^{+0.15} _{-0.12}	-0.56 ^{+0.3} _{-0.36}	0.88±0.176	1.38±0.1
Mrk 79	43.68±0.07	7.84 ^{+0.12} _{-0.16}	-0.68 ^{+0.25} _{-0.21}	0.33±0.066	2.1±0.06
SDSS J074352	45.37±0.02	7.93 ^{+0.05} _{-0.04}	1.69 ^{+0.12} _{-0.13}	1.11±0.222	1.6±0.02
SDSS J075051	45.33±0.01	7.67 ^{+0.11} _{-0.07}	2.14 ^{+0.16} _{-0.24}	1.22±0.244	1.54±0.01
SDSS J075101	44.18±0.09	7.18 ^{+0.08} _{-0.09}	1.39 ^{+0.21} _{-0.21}	0.97±0.194	1.52±0.08
Mrk 382	43.12±0.08	6.5 ^{+0.19} _{-0.29}	1.18 ^{+0.69} _{-0.53}	0.75±0.15	1.74±0.36
SDSS J075949	44.2±0.03	7.44 ^{+0.25} _{-0.25}	0.89 ^{+0.41} _{-0.41}	1.02±0.204	1.49±0.04
SDSS J080101	44.27±0.03	6.78 ^{+0.34} _{-0.17}	2.33 ^{+0.39} _{-0.72}	1.01±0.202	1.61±0.08
SDSS J080131	43.97±0.04	6.51 ^{+0.22} _{-0.17}	2.43 ^{+0.29} _{-0.36}	1.49±0.298	1.36±0.03
PG 0804+761	44.91±0.02	8.43 ^{+0.05} _{-0.06}	0.0 ^{+0.15} _{-0.13}	0.61±0.122	2.13±0.04
SDSS J081441	43.96±0.06	7.18 ^{+0.2} _{-0.2}	1.09 ^{+0.35} _{-0.35}	0.46±0.092	1.54±0.08
SDSS J081456	43.99±0.04	7.44 ^{+0.12} _{-0.49}	0.59 ^{+1.03} _{-0.3}	1.31±0.262	1.71±0.09
NGC 2617	42.67±0.16	7.74 ^{+0.11} _{-0.17}	-1.98 ^{+0.55} _{-0.51}	0.31±0.062	2.55±0.18
SDSS J083553	44.44±0.02	6.87 ^{+0.16} _{-0.25}	2.41 ^{+0.53} _{-0.35}	1.57±0.314	1.73±0.02
SDSS J084533	44.53±0.02	6.76 ^{+0.14} _{-0.15}	2.76 ^{+0.24} _{-0.24}	1.11±0.222	1.38±0.03
PG 0844+349	44.22±0.07	7.66 ^{+0.15} _{-0.23}	0.5 ^{+0.57} _{-0.42}	0.78±0.156	1.79±0.04
SDSS J085946	44.41±0.03	7.3 ^{+0.19} _{-0.61}	1.51 ^{+1.27} _{-0.43}	1.39±0.278	1.59±0.04
Mrk 110	43.66±0.12	7.1 ^{+0.13} _{-0.14}	0.77 ^{+0.26} _{-0.25}	0.14±0.028	1.69±0.09
SDSS J093302	44.31±0.13	7.08 ^{+0.08} _{-0.11}	1.79 ^{+0.4} _{-0.4}	1.44±0.288	1.26±0.02
SDSS J093922	44.07±0.04	6.53 ^{+0.07} _{-0.33}	2.54 ^{+0.71} _{-0.2}	1.48±0.296	1.29±0.06
PG 0953+414	45.19±0.01	8.44 ^{+0.06} _{-0.07}	0.39 ^{+0.16} _{-0.14}	0.27±0.054	1.85±0.04
SDSS J100402	45.52±0.01	7.44 ^{+0.37} _{-0.06}	2.89 ^{+0.13} _{-0.75}	1.17±0.234	1.47±0.01
SDSS J101000	44.76±0.02	7.46 ^{+0.27} _{-0.14}	1.7 ^{+0.31} _{-0.56}	2.17±0.434	1.64±0
NGC 3227	42.24±0.11	7.09 ^{+0.09} _{-0.12}	-1.34 ^{+0.38} _{-0.36}	0.46±0.092	2.44±0.17
SDSS J102339	44.09±0.03	7.16 ^{+0.25} _{-0.08}	1.29 ^{+0.2} _{-0.56}	1.03±0.206	1.48±0.04
Mrk 142	43.59±0.04	6.47 ^{+0.38} _{-0.38}	1.93 ^{+0.59} _{-0.59}	1.14±0.228	1.36±0.26
NGC 3516	42.79±0.2	7.82 ^{+0.05} _{-0.08}	-1.97 ^{+0.41} _{-0.52}	0.66±0.132	2.45±0.17
SBS 1116+583A	42.14±0.23	6.78 ^{+0.11} _{-0.12}	-0.87 ^{+0.51} _{-0.71}	0.59±0.118	2.36±0.13
Arp 151	42.55±0.1	6.87 ^{+0.05} _{-0.08}	-0.44 ^{+0.3} _{-0.28}	0.32±0.064	1.54±0.04
NGC 3783	42.56±0.18	7.45 ^{+0.12} _{-0.11}	-1.58 ^{+0.45} _{-0.59}	0.04±0.008	2.23±0.05
MCG +06-26-012	42.67±0.11	6.92 ^{+0.14} _{-0.12}	-0.34 ^{+0.37} _{-0.45}	1.04±0.208	1.7±0.11

UGC 06728	41.86±0.08	5.87 ^{+0.19} _{-0.4}	0.55 ^{+0.92} _{-0.51}	1.11±0.222	0.89±0.12
Mrk 1310	42.29±0.14	6.62 ^{+0.07} _{-0.08}	-0.31 ^{+0.35} _{-0.39}	0.46±0.092	1.99±0.07
NGC 4051	41.9±0.15	5.72 ^{+0.34} _{-0.44}	0.9 ^{+0.79} _{-0.74}	1.18±0.236	1.97±0.15
NGC 4151	42.09±0.21	7.72 ^{+0.07} _{-0.06}	-2.81 ^{+0.37} _{-0.57}	0.22±0.044	2.76±0.07
PG 1211+143	44.73±0.08	7.87 ^{+0.11} _{-0.26}	0.84 ^{+0.63} _{-0.35}	0.42±0.084	1.35±0.04
Mrk 202	42.26±0.14	6.11 ^{+0.2} _{-0.2}	0.66 ^{+0.59} _{-0.65}	0.57±0.114	1.7±0.08
NGC 4253	42.57±0.12	6.49 ^{+0.1} _{-0.1}	0.36 ^{+0.36} _{-0.42}	0.99±0.198	1.48±0.06
PG 1226+023	45.92±0.05	8.5 ^{+0.03} _{-0.04}	1.37 ^{+0.15} _{-0.14}	0.64±0.128	1.97±0.03
PG 1229+204	43.7±0.05	8.03 ^{+0.24} _{-0.23}	-1.03 ^{+0.52} _{-0.55}	0.53±0.106	2.38±0.05
NGC 4593	42.62±0.37	7.26 ^{+0.09} _{-0.09}	-1.1 ^{+0.6} _{-0.64}	0.89±0.178	2.87±0.66
IRAS F12397+3333	44.23±0.05	6.79 ^{+0.27} _{-0.45}	2.26 ^{+0.98} _{-0.62}	1.48±0.296	1.57±0.52
NGC 4748	42.56±0.12	6.61 ^{+0.11} _{-0.23}	0.1 ^{+0.61} _{-0.44}	0.99±0.198	1.93±0.08
PG 1307+085	44.85±0.02	8.72 ^{+0.13} _{-0.26}	-0.68 ^{+0.53} _{-0.28}	0.21±0.042	2.58±0.09
MCG +06-30-015	41.64±0.11	6.63 ^{+0.12} _{-0.15}	-1.29 ^{+0.37} _{-0.38}	0.93±0.186	2.01±0.08
NGC 5273	41.54±0.16	7.14 ^{+0.19} _{-0.56}	-2.5 ^{+1.33} _{-0.67}	0.58±0.116	3.12±0.13
Mrk 279	43.71±0.07	7.97 ^{+0.09} _{-0.12}	-0.89 ^{+0.33} _{-0.3}	0.55±0.11	2.94±0.03
PG 1411+442	44.56±0.02	8.28 ^{+0.17} _{-0.3}	-0.23 ^{+0.63} _{-0.38}	0.63±0.126	1.58±0.04
NGC 5548	43.3±0.19	8.08 ^{+0.16} _{-0.16}	-1.76 ^{+0.31} _{-0.32}	0.1±0.02	2.66±0.33
PG 1426+015	44.63±0.02	8.97 ^{+0.12} _{-0.22}	-1.51 ^{+0.47} _{-0.28}	0.46±0.092	2.45±0.09
Mrk 817	43.74±0.09	7.99 ^{+0.14} _{-0.14}	-0.87 ^{+0.22} _{-0.22}	0.69±0.138	2.59±0.29
Mrk 1511	43.16±0.06	7.29 ^{+0.07} _{-0.07}	-0.34 ^{+0.24} _{-0.24}	0.8±0.16	2.2±0.13
Mrk 290	43.17±0.06	7.55 ^{+0.07} _{-0.07}	-0.85 ^{+0.23} _{-0.23}	0.29±0.058	2.57±0.18
Mrk 486	43.69±0.05	7.24 ^{+0.12} _{-0.06}	0.55 ^{+0.2} _{-0.32}	0.54±0.108	1.5±0.06
Mrk 493	43.11±0.08	6.14 ^{+0.04} _{-0.11}	1.88 ^{+0.33} _{-0.21}	1.13±0.226	1.52±0.03
PG 1613+658	44.77±0.02	8.81 ^{+0.14} _{-0.21}	-0.97 ^{+0.45} _{-0.31}	0.38±0.076	2.94±0.05
PG 1617+175	44.39±0.02	8.79 ^{+0.15} _{-0.28}	-1.5 ^{+0.58} _{-0.33}	0.74±0.148	2.87±0.12
PG 1700+518	45.59±0.01	8.4 ^{+0.08} _{-0.08}	1.08 ^{+0.17} _{-0.17}	1.32±0.264	1.09±0.08
3C 382	43.84±0.1	8.67 ^{+0.09} _{-0.06}	-2.09 ^{+0.26} _{-0.35}	0.31±0.062	1.87±0.13
3C 390.3	44.43±0.58	9.18 ^{+0.23} _{-0.23}	-2.62 ^{+0.95} _{-0.96}	0.12±0.024	2.62±0.66
KA 1858+4850	43.43±0.05	6.94 ^{+0.07} _{-0.09}	0.75 ^{+0.25} _{-0.21}	0.11±0.022	2.13±0.13
NGC 6814	42.12±0.28	7.16 ^{+0.05} _{-0.06}	-1.64 ^{+0.46} _{-0.8}	0.45±0.09	1.73±0.03
Mrk 509	44.19±0.05	8.15 ^{+0.03} _{-0.03}	-0.52 ^{+0.13} _{-0.14}	0.13±0.026	1.94±0.01
PG 2130+099	44.32±0.04	7.29 ^{+0.06} _{-0.09}	1.4 ^{+0.24} _{-0.19}	0.96±0.192	1.39±0.11
NGC 7469	43.51±0.11	7.6 ^{+0.12} _{-0.06}	-0.46 ^{+0.26} _{-0.42}	0.43±0.086	1.49±0.18

Columns^{††} depict: (1) Source name; (2) luminosity at 5100Å in log-scale; (3) black hole mass in log-scale; (4) dimensionless accretion rate (\dot{M}) in log-scale; (5) the ratio of the EW(Fe II) in the optical within 4434-4684Å to the EW(H β); and (6) ratio of the FWHM(H β) to the $\sigma_{H\beta}$.

^{††}Compiled using the estimates provided in Tables 1 (electronically available also on CDS/Vizier) and 2 in Du and Wang (2019).

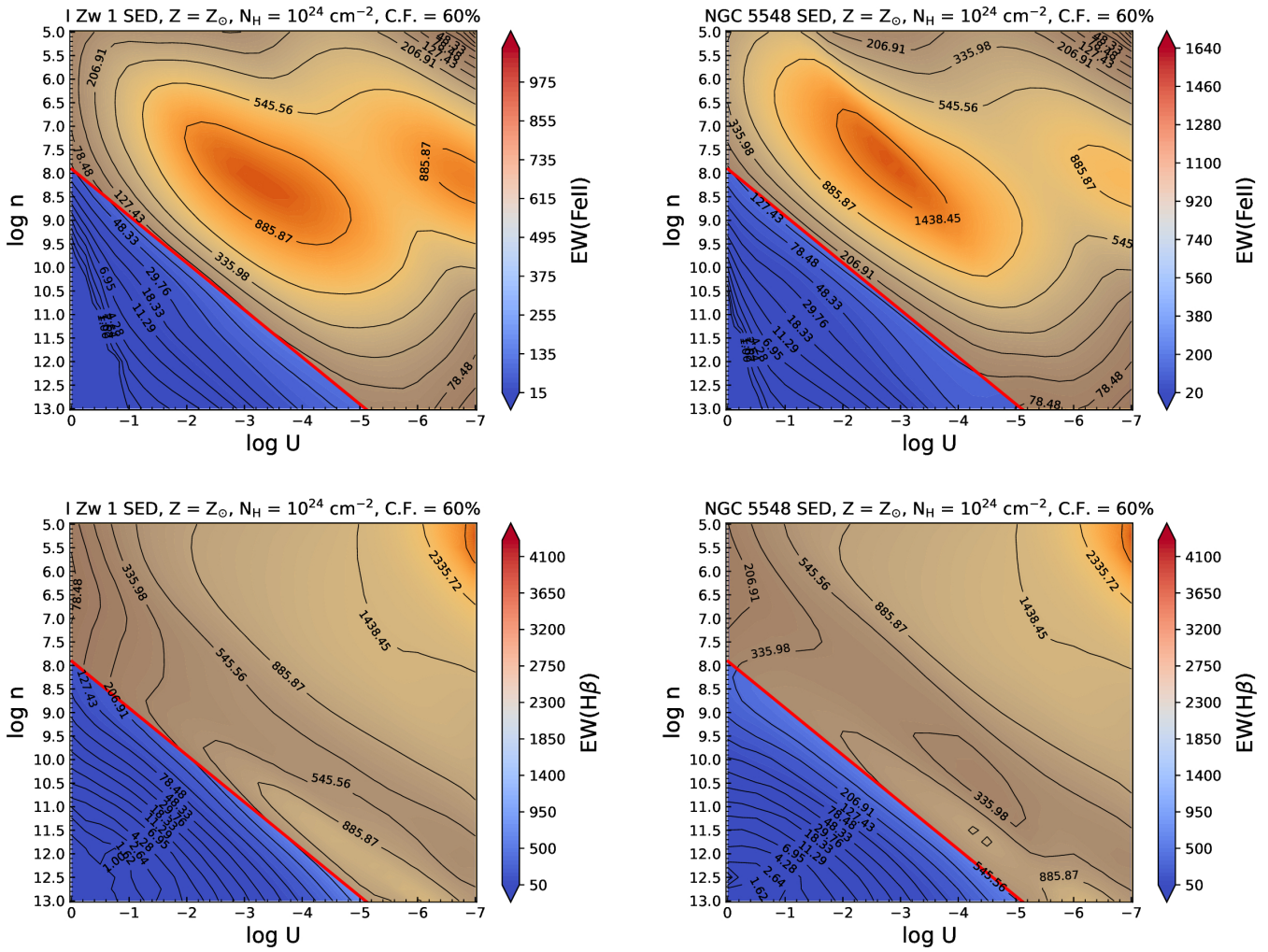


Figure S2. $\log U - \log n_H$ 2D histograms color-weighted by (top panels) equivalent width (EWs) Fe II, and (bottom panels) $EW(H\beta)$. The labels and parameters shown here are identical to Figure 2 except here we use a larger value for the covering fraction, i.e., 60%.